RESEARCH ARTICLE

Amendments to some IEC TR 62095 Recommendations for Underground Single-Core Power Cables in Trefoil Formation

Dardan Klimenta[1], **Marko Sucurovic**[2,*] **and Dragan Tasic**[3]

[1] Faculty of Technical Sciences, University of Priština in Kosovska Mitrovica, RS-38220 Kosovska Mitrovica, Serbia
[2] Faculty of Technical Sciences, University of Kragujevac, RS-32102 Čačak, Serbia
[3] Faculty of Electronic Engineering, University of Niš, RS-18104 Niš, Serbia

Abstract

In the last decade, design engineers have been increasingly required to calculate the ampacities of cable lines using the finite element method (FEM) according to IEC TR 62095, especially for cases that cannot be solved analytically based on IEC 60287. In this regard, CIGRE Study Committee B1 noted in 2020 that there are many gaps in the technical report IEC TR 62095 and then published in 2025 a technical brochure. However, a certain number of those gaps still remained unaddressed. This paper proposes concrete solutions for addressing several gaps related to underground single-core power cables in trefoil formations. 110 kV single-core cables with cross-linked polyethylene insulation are considered, and FEM-based modeling is used for their steady-state thermal analysis. FEM-based models utilized here assume that the cables are installed directly in the dried-out soil, without cable bedding, under the most unfavorable ambient conditions. Appropriate analytical IEC-based models are used to verify the correctness of the proposed solutions. The ampacity obtained using the FEM differs from the corresponding IEC 60287-based value by only -0.263%, and the maximum conductor temperature deviations from the continuously permissible temperature are lower than 0.01 °C. The differences guarantee the reliability of FEM-based calculations.

Keywords: ampacity, finite element method (FEM), power cable, steady-state thermal analysis.

1 Introduction

Nowadays, according to [1], it is common for customers of various power cable systems (underground, submarine, building, urban, etc.) to request that complete ampacity calculations or their parts be carried out using finite element method (FEM), especially in cases where the relevant IEC 60287 standards [2–4] cannot be easily applied. The technical report IEC TR 62095 [5] provides the type of guidance and recommendations needed for ampacity calculations and thermal analysis (steady-state or dynamic) of underground power cables in different formations. However, as noted by CIGRE Study Committee B1 in [1] and some

Submitted: 30 July 2025
Accepted: 04 September 2025
Published: 23 October 2025

Vol. 1, **No.** 1, 2025.
10.62762/TEPNS.2025.641725

***Corresponding author:**
✉ Marko Sucurovic
marko.sucurovic@ftn.kg.ac.rs

Citation
Klimenta, D., Sucurovic, M., & Tasic, D. (2025). Amendments to some IEC TR 62095 Recommendations for Underground Single-Core Power Cables in Trefoil Formation. *ICCK Transactions on Electric Power Networks and Systems*, 1(1), 38–49.

other researchers in their studies [6–8], this technical report has not been updated since its publication and does not meet a certain number of basic needs of modern users. Most of these gaps were filled by CIGRE in the technical brochure [1], but only with partial scientific explanations. Moreover, some of the gaps remained unaddressed, or have not yet been recognized by CIGRE. This acted as a motivation to propose amendments of some recommendations from IEC TR 62095 [5].

Specifically, the research results from [6] showed that for the purposes of steady-state and dynamic thermal analyses of underground power cables, the ground surface can be modeled by the forced convection boundary condition, while the bottom edge of the computational domain can be modeled by the constant temperature boundary condition. In addition, in this study, computational domains significantly larger than the 10 m × 5 m domain recommended by IEC TR 62095 [5] were considered, it was noted that this technical report neglects the thermal effects of solar radiation on underground power cables, and everything was validated by means of experimentation. To simplify thermal modeling, the authors of [7] assumed that all losses are generated in cable conductors, that the heat from the ground surface to the ambient air transfers by natural convection, and that the size of the computational domain is 10 m × 10 m. All these assumptions were also validated by experimentation, and do not correspond with the recommendations of IEC TR 62095 [5]. The effects of the solar heat, computational domain size, heat source models and convective-radiative ground surface on the temperatures of underground power cables and their surroundings were analyzed in [8]. According to [9], FEM-based modeling of underground power cables can be memory-intensive and time-consuming. The effects of computational domains larger than 10 m × 5 m and various combinations of boundary conditions were considered in [10], including experimental validation of the obtained results. A computational domain having external dimensions of 20 m × 10 m was used in [11] for a cost-benefit analysis of investments in underground cable systems. The effect of metallic screen bonding design on heat sources in metallic screens of a cable line was modeled in [12]. In [12], the computational domain was 40 m × 20 m, while the ground surface was represented by a constant temperature or forced convection boundary condition. Reference [13] proposed a FEM-based approach for calculating the external thermal resistance of a power cable in non-homogeneous soil using a simplification from IEC TR 62095. In all the publications reviewed here, the authors deviated substantially from the IEC TR 62095 recommendations, but their results were validated experimentally and/or verified using appropriate analytical IEC-based models. All this implies a need to amend certain recommendations, that is, fill some existing gaps of IEC TR 62095.

This paper addresses the existing gaps in the technical report IEC TR 62095 regarding three single-core power cables installed directly into the dried-out soil, in trefoil formation. It is assumed that the cables are of the type ABB AXLJ 1×1000/190 mm^2 110 kV, with cross-linked polyethylene (XLPE) insulation and cross-bonding of their metallic screens. In addition, it is assumed that the cable line has a balanced three-phase load. The steady-state thermal analysis of the underground cable line is performed using appropriate FEM-based models created in COMSOL 4.3 Heat Transfer Module [14]. These FEM-based models assume that operating conditions are normal and that ambient conditions are the most unfavorable. In particular, this paper will address the gaps of IEC TR 62095 regarding the following steps of FEM-based steady-state thermal modeling: (i) selection of the external dimensions of a computational domain; (ii) specifying boundary conditions at the external edges of a computational domain; (iii) modeling heat sources in conductors and insulation layers; and (iv) checking the accuracy of a FEM-based model by means of finite element (FE) mesh independence tests. All proposed solutions for addressing the gaps of IEC TR 62095 can be regarded as scientific and engineering contributions of this study. Finally, verification of the correctness of the proposed solutions built in the FEM-based steady-state thermal models is carried out with the help of appropriate IEC 60287-based models.

2 Case Study

Figure 1 illustrates a computational domain for the case when three single-core power cables of the type ABB AXLJ 1×1000/190 mm^2 110 kV are laid in trefoil formation, directly in the dried-out soil. Figure 1(a) shows the computational domain, i.e., case study that will be utilized in this paper, while Figure 1(b) shows the dimensions of the construction elements of the considered 110 kV cables. The parameters appearing in Figure 1 have the following meanings: W is the width of the computational domain in m, D is the vertical dimension of the computational domain in m, L is the

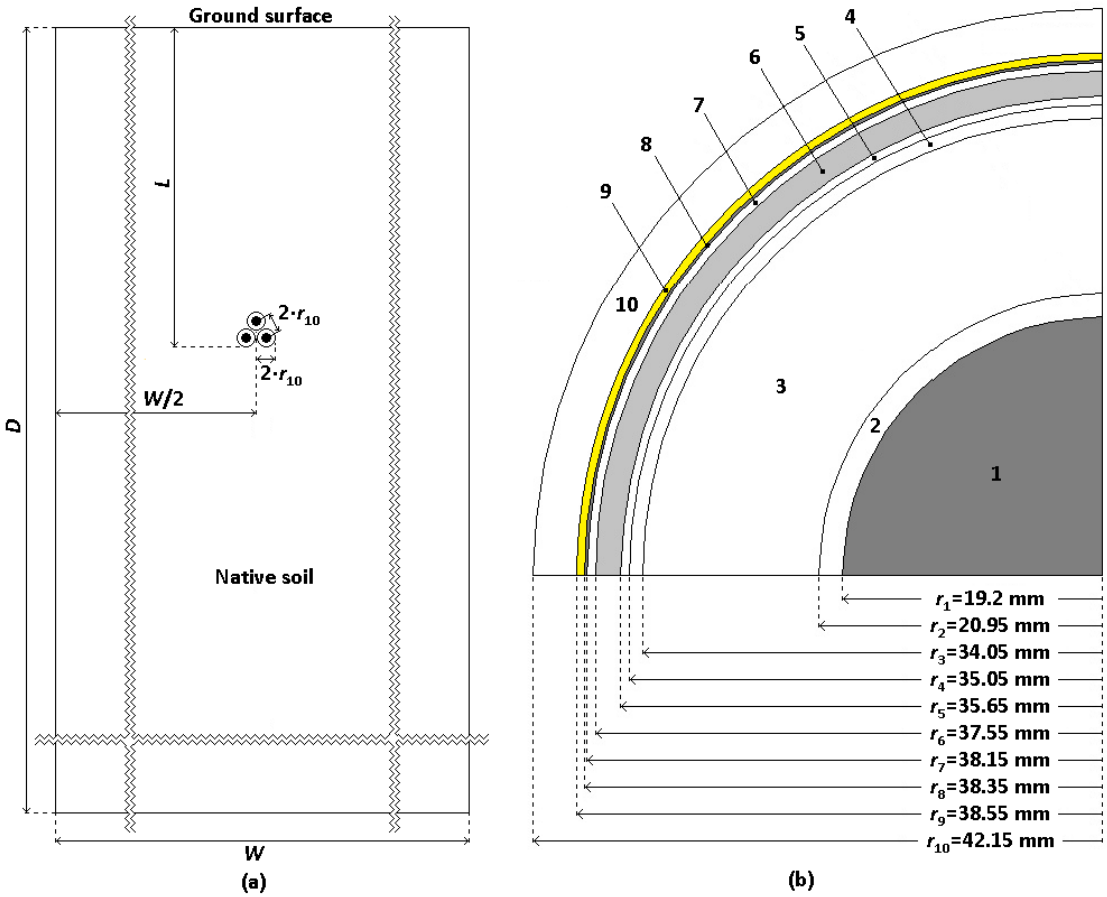

Figure 1. Representation of the considered case study; (a) Computational domain with a 110 kV underground cable line; and (b) Dimensions of the construction elements of the ABB AXLJ 1×1000/190 mm^2 110 kV cable, i.e., radii of 1 – aluminum conductor, 2 – semi-conducting XLPE screen over the conductor, 3 – XLPE insulation, 4 – semi-conducting XLPE screen over the insulation, 5 – semi-conducting PE swelling tapes under the copper screen, 6 – copper screen with the rated cross-sectional area of 190 mm^2, 7 – semi-conducting PE swelling tapes over the copper screen, 8 – radial water-sealing aluminum layer, 9 – conducting HDPE layer, and 10 – outer HDPE sheath.

cable line laying depth in m, and r_i for $i = 1, 2, \ldots, 10$ is the radius of the i-th cable construction element in mm.

For the purpose of FEM-based steady-state thermal analysis in COMSOL 4.3, according to [15], the AXLJ 1×1000/190 mm^2 110 kV cable needs to be modeled with an equivalent design having the aluminum conductor, XLPE insulation, metallic screen and outer high density polyethylene (HDPE) sheath with outer radii r_1, r_5, r_8 and r_10, respectively. This means that the semi-conducting screens and swelling tapes under the copper screen are added to equivalent XLPE insulation; that the swelling tapes over the copper screen and water-sealing aluminum layer are included in an equivalent metallic screen; and that the conducting HDPE layer is added to an equivalent outer HDPE sheath. Thermal conductivities of these equivalent construction elements are: k_c=239 W/(Km) – for the aluminum conductor, k_d=0.286 W/(Km) – for the equivalent XLPE insulation, k_{sc}=385 W/(Km) – for the equivalent metallic screen, and k_{sh}=0.245 W/(Km) – for the equivalent outer HDPE sheath. The equivalent cable construction is created in accordance with the following IEC 60287-1-1 guidance [2]: "Where screening layers are present, for thermal calculations metallic tapes are considered to be part of the conductor or sheath while semi-conducting layers (including metallized carbon paper tapes) are considered as part of the insulation. The appropriate component dimensions must be modified accordingly." According to [12], the thermal conductivity of the equivalent metallic screen is taken to be equal to the thermal conductivity of copper. Since the swelling tapes over the copper screen are included in the equivalent metallic screen, it means that the thermal resistance of these swelling tapes was added to the thermal resistance of the outer HDPE sheath, that is, the thermal conductivity k_{sh} represents the equivalent thermal conductivity of the outer HDPE sheath [12].

Since it is assumed that the metallic screens are cross-bonded and that loads in the phase cables are mutually equal and balanced, there will be no heat sources in equivalent metallic screens. In the given case, heat sources will exist in aluminum conductors and equivalent layers of XLPE insulation. Although Standard 60287-1-1 [2] recommends that dielectric losses do not need to be taken into account for values of the phase-to-phase voltages lower than or equal to 110 kV, they are included in all numerical and analytical calculations. Consequently, only the electrical resistivity of aluminum at 20 °C (which is $\rho_{\mathrm{Al}} = 2.8264 \cdot 10^{-8}\,\Omega \cdot \mathrm{m}$) is required for the calculation of heat sources in aluminum conductors.

From the most unfavorable ambient conditions specified in [15], the following conditions will be used or mentioned here: (i) temperature of the air along the ground surface of $T_a = 40\,^{\circ}\mathrm{C}$; (ii) solar irradiance $Q_{S,s} = 1000\,\mathrm{W/m^2}$; (iii) temperature of the reference soil $T_{\mathrm{rs}} = 20\,^{\circ}\mathrm{C}$; and (iv) thermal conductivity of the native soil whose value corresponds to its dried-out state, that is, $k_{\mathrm{ns}} = 0.4\,\mathrm{W/(K \cdot m)}$. In addition, it is assumed that the ground surface is covered with dry grass. According to [8], the thermal emissivity and solar absorptivity corresponding to such a ground surface are $\varepsilon = 0.94$ and $\alpha = 0.6$, respectively.

3 FEM-Based Steady-State Thermal Modeling

Two-dimensional steady-state thermal analysis of the case study represented by the computational domain in Figure 1(a) is governed by the following partial differential equation [8, 12]:

$$\nabla \cdot (-k\nabla T) = \frac{\partial}{\partial x}\left(-k\frac{\partial T}{\partial x}\right) + \frac{\partial}{\partial y}\left(-k\frac{\partial T}{\partial y}\right) = Q_v \tag{1}$$

where T is the unknown nodal temperature in K; k is the thermal conductivity in $\mathrm{W/(K \cdot m)}$; x and y are the Cartesian spatial coordinates in m; and Q_v is the volume power of heat sources in $\mathrm{W/m^3}$. Depending on whether or not a radiation boundary condition exists in a FEM-based model used, that model will be nonlinear or linear, respectively.

The volume power of heat sources in aluminum conductors with a radius of $r_1 = 0.0192\,\mathrm{m}$ and a geometric cross-sectional area of $S_c' = 1158.117 \cdot 10^{-6}\,\mathrm{m^2}$ is [8, 15].

$$Q_{c,v} = \frac{R_{\mathrm{ac}}(T_{\mathrm{cp}})}{S_c'} \cdot I^2 \tag{2}$$

where $R_{\mathrm{ac}}(T_{\mathrm{cp}}) = 4.102127 \cdot 10^{-5}\,\Omega/\mathrm{m}$ is the ac resistance of one conductor per unit length of the cable at temperature T_{cp}, calculated in accordance with IEC 60287-1-1 [2] and IEC 60228 [16]; $T_{\mathrm{cp}} = 90\,^{\circ}\mathrm{C}$ is the continuously permissible temperature of XLPE-insulated cables; and I is the cable ampacity or load current in A. Also, it should be noted that in Equation (2), the geometric and not the rated or effective cross-sectional area of the conductors must be used. The effective cross-sectional area of the conductors was used to obtain the ac resistance $R_{\mathrm{ac}}(T_{\mathrm{cp}})$.

The volume power of heat sources in equivalent insulation layers $Q_{d,v}$ in $\mathrm{W/m^3}$ is given by [12, 15]:

$$Q_{d,v} = \frac{Q_{d,l}}{\pi(r_5^2 - r_1^2) \cdot 10^{-6}} \tag{3}$$

where $Q_{d,l} = 0.362647\,\mathrm{W/m}$ is the dielectric loss per unit length of the cable, and $\pi(r_5^2 - r_1^2) \cdot 10^{-6}$ is the geometric cross-sectional area of one equivalent insulation layer in $\mathrm{m^2}$.

The upper edge of the computational domain in Figure 1(a) representing the ground surface is modeled by

$$T = T_{rs} \tag{4}$$

- Dirichlet boundary condition of constant temperature, or by a combination of the following boundary conditions:

$$\vec{n} \cdot (-k\nabla T) = -\alpha \cdot Q_{S,s} \tag{5}$$

- Neumann boundary condition of constant heat flux,

$$\vec{n} \cdot (-k\nabla T) = h_c(T - T_{rs}) \tag{6}$$

- Robin boundary condition of convection heat transfer, and

$$\vec{n} \cdot (-k\nabla T) = \varepsilon \cdot \sigma_{\mathrm{SB}} \cdot T^4 \tag{7}$$

- Stefan-Boltzmann boundary condition of radiation heat transfer [8, 12, 15]. In addition, the left- and right-hand edges of the computational domain in Figure 1(a) are modeled by Equation (4) or

$$\vec{n} \cdot (-k\nabla T) = 0 \tag{8}$$

- Neumann boundary condition of thermal insulation [8, 12, 15]. While, the bottom edge of the computational domain in Figure 1(a) is represented by Equation (4) or Equation (8) in accordance with [6, 12]. In Equations (4-8), T is the unknown temperature of the ground surface in K; T_{rs} is the known temperature of the ground surface or the known temperature of the air along the ground surface in K [2, 5, 12]; $\vec{n}$ is the outwards-oriented normal vector of the Neumann, Robin and Stefan-Boltzmann boundaries; h_c is the convection heat transfer coefficient in $\mathrm{W}/(\mathrm{m}^2 \cdot \mathrm{K})$; and $\sigma_{\mathrm{SB}} = 5.67 \cdot 10^{-8}\,\mathrm{W}/(\mathrm{m}^2 \cdot \mathrm{K}^4)$ is the Stefan-Boltzmann constant.

4 Results and Discussion

4.1 Selection of the Size of a Computational Domain

To demonstrate the correct selection of the external dimensions of a computational domain, the two different FEM-based steady-state thermal models with 110 kV cables were created and analyzed. For both models, it is assumed that the ambient and boundary conditions correspond with the ones of IEC 60287. Figure 2(a) shows the steady-state temperature distribution over the $10\,\mathrm{m} \times 5\,\mathrm{m}$ computational domain (recommended in IEC TR 62095), while Figure 2(b) shows the steady-state temperature distribution over the $40\,\mathrm{m} \times 21.5\,\mathrm{m}$ computational domain (recommended in Reference [15]). The temperature distributions over these domains are also calculated for: the cable line laying depth of $L = 1.5\,\mathrm{m}$; the volume powers of heat sources in conductors and insulation layers of $Q_{c,v} = 12430.8\,\mathrm{W/m^3}$ and $Q_{d,v} = 127.936\,\mathrm{W/m^3}$, respectively; the isothermal Dirichlet boundary condition $T = T_{rs} = 20\,^{\circ}\mathrm{C}$ on the ground surface; and the homogeneous (i.e., adiabatic) Neumann boundary condition on the left-hand, bottom and right-hand edges of the computational domains.

Based on Figure 2(a), for the computational domain of dimensions $10\,\mathrm{m} \times 5\,\mathrm{m}$, the maximum conductor temperature of 92.323 °C was obtained, which is 2.323 °C or 2.581% higher than the continuously permissible temperature $T_{\mathrm{cp}} = 90\,^{\circ}\mathrm{C}$. This result cannot be considered reliable. In addition, the isotherm of 30 °C is not a closed contour, which is not in agreement with the relevant data from [17] whose accuracy was validated by appropriate experiments. Moreover, when the constant temperature boundary condition $T = T_{\mathrm{rs}} = 20\,^{\circ}\mathrm{C}$ is used instead of the adiabatic boundary condition on the left-hand, bottom and right-hand edges, the maximum conductor temperature is 87.304 °C, which is -2.696 °C or -2.995% lower than $T_{\mathrm{cp}} = 90\,^{\circ}\mathrm{C}$. For these reasons, the computational domain with the dimensions recommended by IEC TR 62095 cannot be used for FEM-based steady-state thermal analyses. Furthermore, according to Equation (2) and Figure 2(b), the ampacity $I = 592.408\,\mathrm{A}$ corresponds to the volume power of heat sources in conductors $Q_{c,v} = 12430.8\,\mathrm{W/m^3}$. While based on IEC 60287, the following values for these parameters were obtained: $I = 593.972\,\mathrm{A}$ and $Q_{c,v} = 12496.5\,\mathrm{W/m^3}$. Thus, the ampacity obtained using the FEM-based model in Figure 2(b) differs from the value obtained using the corresponding IEC 60287-based model by only -1.564 A or -0.263%, which goes to the safe side of the calculation.

Reducing the differences between successive ampacity calculations corresponding to computational domains of different sizes to some minor values was used as a criterion for selecting the external domain dimensions by CIGRE in the technical brochure [1]. By using such a criterion in [1], a computational domain of $40\,\mathrm{m} \times 20\,\mathrm{m}$ was selected, which is vertically smaller by 1.5 m than the one recommended more than a decade ago in [15]. Regarding the aforementioned criterion, the technical brochure [1] states the following: "The slight variations observed up to $40\,\mathrm{m} \times 20\,\mathrm{m}$ scenario might be attributed to differences in meshing rather than any impact from the boundaries. Hence, for subsequent cases, a dimension of $40\,\mathrm{m} \times 20\,\mathrm{m}$ has been chosen." This cannot be considered a scientific justification for the selection made. If now in the FEM-based model from Figure 2(b) the left-hand, bottom and right-hand boundaries are isothermal instead of adiabatic, with temperature $T = T_{\mathrm{rs}} = 20\,^{\circ}\mathrm{C}$, the maximum conductor temperature can be 89.708 °C, which is only 0.292 °C lower than the continuously permissible temperature $T_{\mathrm{cp}} = 90\,^{\circ}\mathrm{C}$. This represents a minor difference and shows that for two different types of boundary conditions on the left-hand, bottom and right-hand boundaries, the maximum conductor temperature is negligibly lower than or equal to the continuously permissible temperature. Therefore, the external dimensions of a computational domain must be selected with respect to the continuously permissible temperature and ampacity, and not only with respect to the ampacity. The external left-hand, bottom and right-hand adiabatic or isothermal boundaries must also, with regard to the blocks of a FEM-based model with heat sources, finally be placed at a distance from

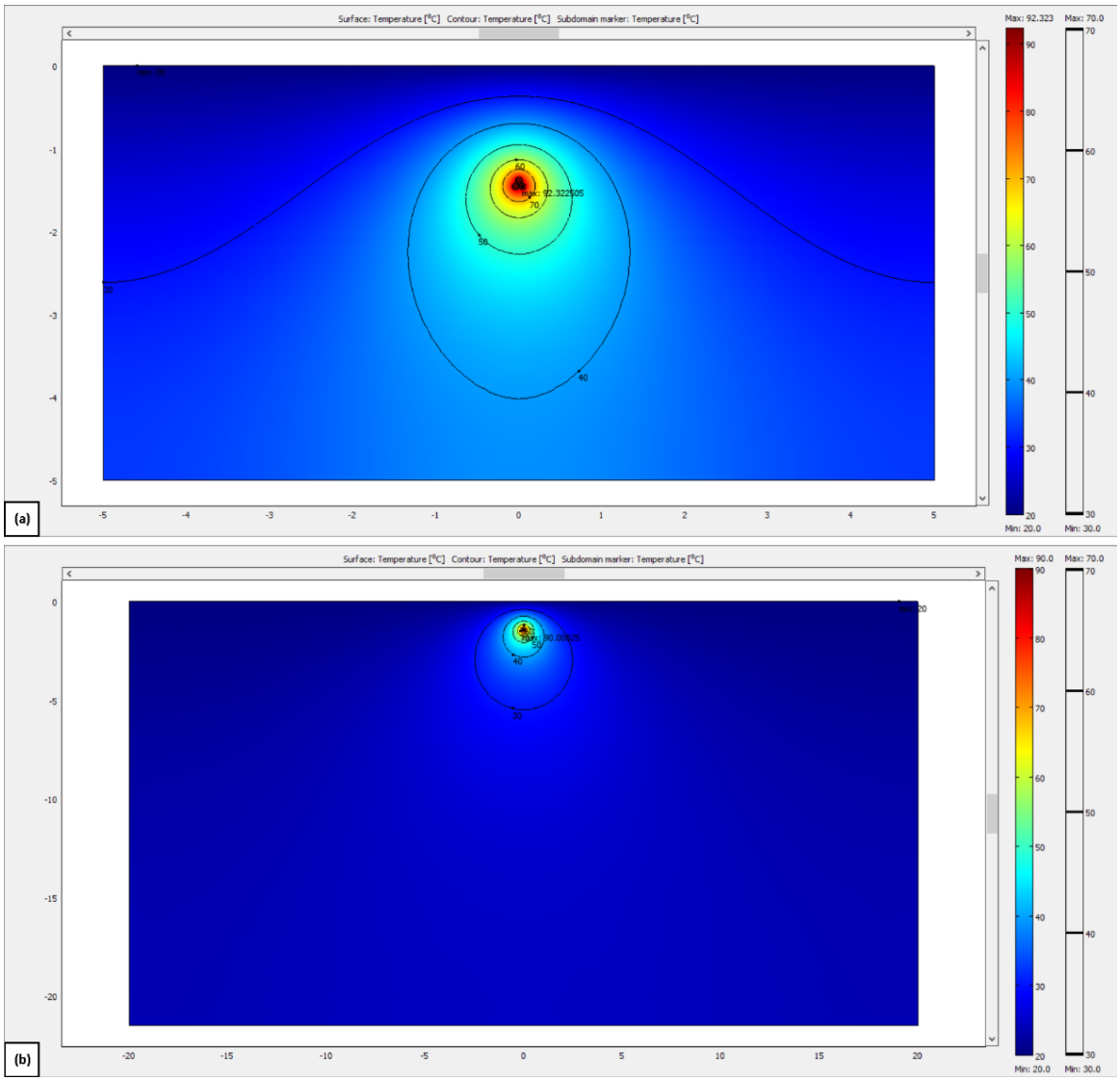

Figure 2. Steady-state temperature distribution and isotherms of 30, 40, 50, 60 and 70 °C generated for the ambient and boundary conditions corresponding to the ones of IEC 60287 and a computational domain with a size of (a) 10 m × 5 m recommended in IEC TR 62095; and (b) 40 m × 21.5 m recommended in [15].

which they will not be able to significantly affect the maximum temperature of those blocks. This is the only acceptable way to select the external dimensions of any computational domain for FEM-based steady-state thermal analyses.

4.2 Specifying Boundary Conditions

After selecting the external dimensions of the computational domain, the next thing to do is to select and specify the best combination of boundary conditions for its edges, of course, again assuming that the thermal conductivities of materials and heat sources within those materials are correctly specified. Combinations of boundary conditions that yield cable ampacities identical or close to those calculated using the corresponding IEC 60287-based models (which were already validated experimentally by many researchers) are the correct ones to use in FEM-based steady-state thermal modeling. The ground surface can be modeled with a constant temperature boundary, a forced convection boundary condition, or a combination of forced convection and radiation boundary conditions. The remaining boundaries can be isothermal or adiabatic. The assumption that the bottom edge of the computational domain can be represented by a boundary condition of constant temperature equal to the temperature of the reference soil was experimentally validated in [6]. Accordingly, this study considers scenarios with combinations of boundary conditions where the left- and right-hand boundaries are adiabatic and the bottom boundary is isothermal.

In all these combinations of boundary conditions,

Table 1. Maximum conductor temperature and details on the shape of isotherms obtained for various combinations of boundary conditions on the external edges of the 40 m × 21.5 m computational domain.

Scenario	Boundary condition on the upper edge	Boundary condition on the bottom edge	Boundary condition on the left- and right-hand edges	Max. conductor temperature in °C	Shape of isotherms
A	Constant temperature *Trs*=20 °C	Homogeneous	Homogeneous	90	Vertical ellipses or circular contours, pushed downwards [a]
B	Constant temperature *Trs*=20 °C	Constant temperature *Trs*=20 °C	Constant temperature *Trs*=20 °C	89.708	Vertical ellipses or circular contours, pushed downwards [a]
C	Constant temperature *Trs*=20 °C	Constant temperature *Trs*=20 °C	Homogeneous	89.726	Vertical ellipses or circular contours, pushed downwards [a]
D	Convection [b]	Homogeneous	Homogeneous	90.02	Vertical ellipses or circular contours, pushed downwards [a]
E	Convection [b]	Constant temperature *Trs*=20 °C	Constant temperature *Trs*=20 °C	89.727	Vertical ellipses or circular contours, pushed downwards [a]
F	Convection [b]	Constant temperature *Trs*=20 °C	Homogeneous	89.745	Vertical ellipses or circular contours, pushed downwards [a]
G	Convection [b] and radiation [c]	Homogeneous	Homogeneous	90.828	Vertical ellipses or circular contours, pushed downwards [a]
H	Convection [b] and radiation [c]	Constant temperature *Trs*=20 °C	Constant temperature *Trs*=20 °C	90.468	Vertical ellipses or circular contours, pushed downwards [a]
I	Convection [b] and radiation [c]	Constant temperature *Trs*=20 °C	Homogeneous	90.499	Vertical ellipses or circular contours, pushed downwards [a]
J	Convection [b] and radiation [d]	Homogeneous	Homogeneous	90	Vertical ellipses or circular contours, pushed downwards [a]
K	Convection [b] and radiation [d]	Constant temperature *Trs*=20 °C	Constant temperature *Trs*=20 °C	89.709	Vertical ellipses or circular contours, pushed downwards [a]
L	Convection [b] and radiation [d]	Constant temperature *Trs*=20 °C	Homogeneous	89.726	Vertical ellipses or circular contours, pushed downwards [a]

[a] Isotherms of 30, 40, 50, 60 and 70 °C pushed axially downwards relative to the ground surface in the same or approximately the same way as in Figure 2(b).
[b] With the convection heat transfer coefficient *hc*=250 W/(m^2×K) and the temperature of the air along the ground surface of *Ta*=*Trs*=20 °C.
[c] With the inward heat flux -*a*×*QS*,*s*=600 W/m^2 and the temperature of the air along the ground surface of *Ta*=*Trs*=20 °C.
[d] With the inward heat flux -*a*×*QS*,*s*=388.6 W/m^2 and the temperature of the air along the ground surface of *Ta*=*Trs*=20 °C.

the temperatures of the ground surface, ambient air and natural soil must be equal to the temperature of the reference soil to obtain a solution identical to that of the corresponding IEC 60287-based model. For the radiation boundary condition, the following two scenarios are considered: (i) that the inward heat flux is equal to $-\alpha \cdot Q_{S,s} = 600\,\mathrm{W/m^2}$ and corresponds to the maximum value of solar irradiance from the most unfavorable ambient conditions, and (ii) that the inward heat flux is lower than $-\alpha \cdot Q_{S,s} = 600\,\mathrm{W/m^2}$ and that its value does not affect the energy balance at the ground surface. The temperature distributions over the $40\,\mathrm{m} \times 21.5\,\mathrm{m}$ computational domain in Figure 1(a) are calculated for: the cable line laying depth of $L = 1.5\,\mathrm{m}$, as well as the volume powers of heat sources in conductors and insulation layers of $Q_{c,v} = 12430.8\,\mathrm{W/m^3}$ and $Q_{d,v} = 127.936\,\mathrm{W/m^3}$, respectively. Table 1 provides the maximum conductor temperature and details on the shape of isotherms obtained for various combinations of boundary conditions on the external edges of the $40\,\mathrm{m} \times 21.5\,\mathrm{m}$ computational domain.

Based on Table 1, the combination of boundary conditions corresponding to Scenario A is the one that should be applied in FEM-based steady-state thermal analyses, although all other combinations also result in maximum conductor temperatures that are very close to the continuously permissible temperature $T_{\mathrm{cp}} = 90\,^{\circ}\mathrm{C}$. In this particular case, the boundary conditions corresponding to Scenario A were selected because the maximum conductor temperature deviation is equal to zero. Practically, this means that at distances equal to or greater than 20 m, the mutual thermal effects of the construction elements of the three cables and the reference soil are negligible in a steady-state. The largest deviation was obtained for Scenario G where the radiation boundary condition was applied (taken from the most unfavorable ambient conditions). In addition, almost half of this deviation was obtained

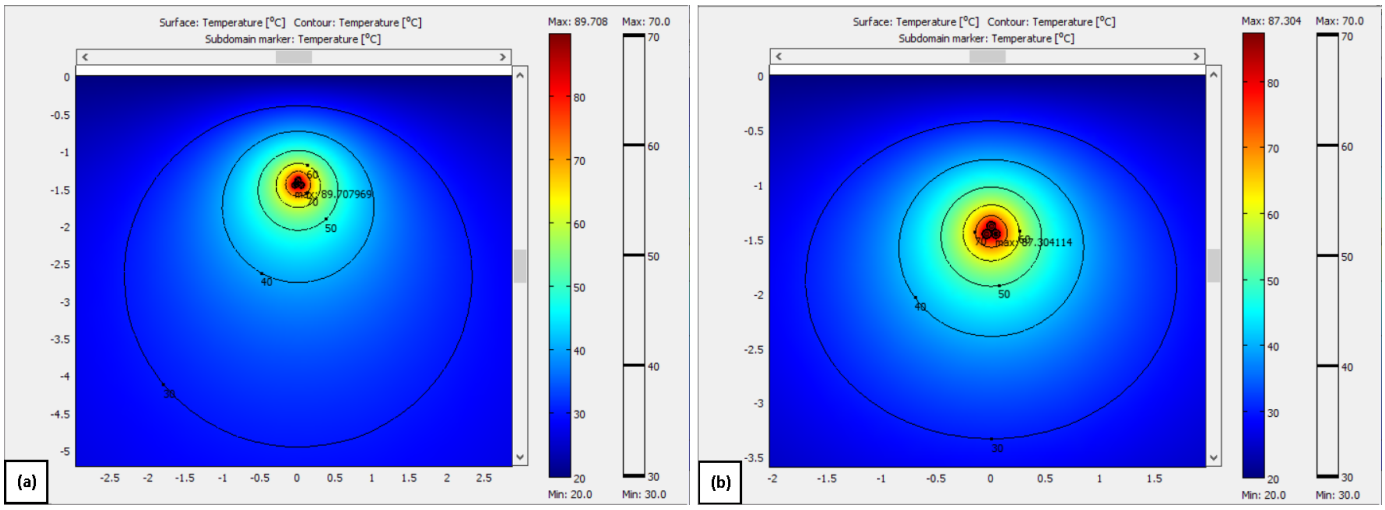

Figure 3. Steady-state temperature distributions over (a) the part of the 40 m × 21.5 m computational domain, and (b) the part of the 10 m × 5 m computational domain, generated for the same isothermal boundary condition on all the external edges, i.e., for Scenario B.

for Scenarios H and I. Such deviations could be expected. Specifically, under the most unfavorable ambient conditions, the solar irradiance of 1000 W/m^2 corresponds to the temperature of the air along the ground surface of 40 °C. This means that the solar irradiance corresponding to the temperature of the air of 20 °C was unknown. By gradually reducing the value of the inward heat flux $-\alpha \cdot Q_{S,s}$ in Equation (5) of the appropriate FEM-based model, it was found that the unknown solar irradiance is $Q_{S,s} = 647.7\,\mathrm{W/m^2}$, which certainly makes sense for $\alpha = 0.6$ and corresponds with a maximum conductor temperature of 90 °C. In particular, the inward heat flux $-\alpha \cdot Q_{S,s}$ was reduced until the same FEM-based model provided the maximum conductor temperature equal to the continuously permissible temperature T_{cp}. Simulations of Scenarios J, K and L with the solar irradiance of $Q_{S,s} = 647.7\,\mathrm{W/m^2}$ showed that in FEM-based steady-state thermal modeling of underground power cables, a radiation boundary condition can also be used, but together with the forced convection boundary condition ($h_c = 250\,\mathrm{W/(m^2 \cdot K)}$ and $T_a = T_{\mathrm{rs}}$). Obviously, the solar irradiance $Q_{S,s} = 647.7\,\mathrm{W/m^2}$ corresponds to the temperature of the air $T_a = 20\,^{\circ}\mathrm{C}$ and the assumption that the ground surface is grey. In general, a combination of forced convection and radiation boundary conditions can be used for underground power cables above which the ground surface is painted, for example, white or light blue to eliminate the urban heat island effect [8]. In particular, modeling the external edges of a computational domain with a combination of boundary conditions that includes a radiation boundary condition was not considered by IEC in [5] or CIGRE in [1].

Finally, it should be shown how it was established that all the isotherms obtained for the scenarios from Table 1 have the correct shapes. According to [17], isotherms surrounding underground power cables should be vertical ellipses or approximately circular contours whose centers move away from the ground surface as their temperature decreases. This was experimentally validated in [17]. Isotherms that are not vertical ellipses or approximately circular contours and do not follow this law can be regarded as incorrect solutions. Figure 3(a) shows the correct solution corresponding to Scenario B from Table 1, and Figure 3(b) shows an incorrect solution obtained using the FEM-based steady-state thermal model from Figure 2(a) for Scenario B. Specifically, the 30 °C isotherm is a horizontal ellipse, and that shape is not allowed, and the like.

4.3 Modeling Heat Sources in Cable Construction Elements

Subsection 3.4 of the technical report IEC TR 62095 [5] only states that FEM-based thermal models, both steady-state and dynamic, should include losses in conductors, insulation layers and metallic screens, as well as their time and/or temperature dependences. Therefore, in the technical report IEC TR 62095 [5] there are no appropriate formulas and recommendations on how it should be carried out. In addition, the technical brochure CIGRE TB 963 [1] recommends the use of relevant formulas from IEC 60287 [2–4] and other IEC standards, and some of those formulas are taken and repeated in the case studies considered. In addition to the formula for calculating power losses generated in conductors

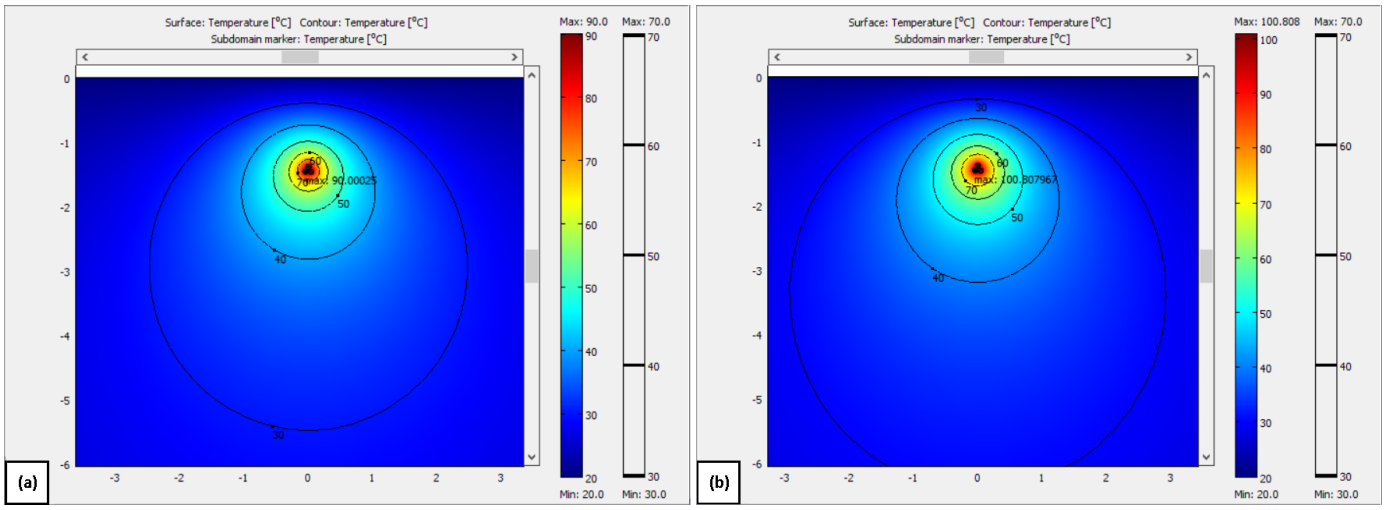

Figure 4. Steady-state temperature distributions over the part of the 40 m × 21.5 m computational domain: (a) Correct solution generated for the volume power of heat sources in conductors of 12430.8 W/m^3; and (b) Incorrect solution generated for the volume power of heat sources in conductors of 14396.3 W/m^3.

Table 2. Results of FE meshes independence tests performed using the FEM-based models from Figures 2(a) and 2(b) for Scenario A.

Computational domain	Finite element mesh						Maximum temperature deviation from T_{cp} in °C
	Automatically generated		After the first refinement		After the second refinement		
	Number of nodes	Number of elements	Number of nodes	Number of elements	Number of nodes	Number of elements	
10 m × 5 m	2704	5352	10759	21408	42925	85632	+2.328
40 m × 21.5 m	2705	5331	10740	21324	42803	85296	+0.009

and Guidance Point 35 relating to heat sources, the technical brochure CIGRE TB 963 [1] highlights the following very important details: the cross-sectional area S'c appearing in Equation (2) represents "the cross-sectional area of the conductor as it is defined in the geometry of the model, which is needed for the unit adaptation to W/m3", and "it is important to ensure the accuracy of the total heat per unit length". In the technical brochure [1], similar statements can be found for the cross-sectional areas of metallic screens and insulation layers. In general, the technical report IEC TR 62095 [5] and the technical brochure CIGRE TB 963 [1] are missing a sentence such as this one: Power losses generated in the conductor, insulation and metallic screen per unit length of one single-core cable must be calculated for their effective (actual) cross-sectional areas in accordance with the relevant IEC standard, while the volume powers of heat sources in them must be recalculated for the corresponding geometric cross-sectional areas, taking care that the losses per unit length remain unchanged.

As for cable conductors, they have their rated, effective/actual and geometric cross-sectional areas. Electrical calculations use the effective cross-sectional area to determine power losses in conductors per unit length, while thermal calculations use the geometric cross-sectional area to determine volume powers of heat sources in conductors. For the geometric cross-sectional area and the ampacity of $I = 592.408$ A (numerical solution obtained using COMSOL), the volume power of heat sources in conductors of $Q_{c,v} = 12430.8\,\mathrm{W/m^3}$ was previously calculated – the correct solution from Subsection 4.2. If the effective cross-sectional area is not known, then the rated one can be used in electrical calculations. In this case, the effective cross-sectional area equals the rated one. With the same ampacity ($I = 592.408$ A), this gives a volumetric heat generation rate of $Q'_{c,v} = 14396.3\,\mathrm{W/m^3}$, which is incorrect. Applying the correct ($Q_{c,v} = 12430.8\,\mathrm{W/m^3}$) and incorrect ($Q'_{c,v} = 14396.3\,\mathrm{W/m^3}$) rates to the FEM model in Figure 2(b) yields the steady-state temperature distributions shown in Figures 4(a) and 4(b). The former represents the correct solution, while the latter shows the erroneous case, with Figure 4(a) depicting the isotherms in the relevant region of the computational domain.

According to Figure 4(b), the incorrect temperature

distribution provided the maximum conductor temperature of 100.808 °C, which is 10.808 °C or 12 % higher than $T_{\mathrm{cp}} = 90$ °C. This specifically means that in the two analyzed cases the power losses generated in the conductor per unit length of each single-core cable are not the same as required. In the case of Figure 4(a), these losses amount to 14.396 W/m, and in the case of Figure 4(b), 16.673 W/m. Thus, the difference between the volume powers of heat sources in conductors of about 2 kW/m^3 causes a significant difference in the conductor temperature that cannot be ignored.

Since, according to IEC 60287-1-1 [2], dielectric losses can be neglected for 110 kV cables, this means that the volume power of heat sources corresponding to these losses (amounting to 127.936 W/m^3) could be used to define permissible deviations for the maximum conductor temperature and the ampacity. If it is assumed that the dielectric losses, in the FEM-based model in Figure 2(b), are zero, the maximum conductor temperature is 88.353 °C. This means that the volume power of heat sources in conductors can be increased from 12430.8 W/m^3 to 12730.3 W/m^3, and the corresponding ampacity can be increased from 592.408 A to 599.502 A. Accordingly, when taking into account dielectric losses, the permissible deviations for the maximum conductor temperature and the ampacity of the considered 110 kV cables could be up to +1.83 % and +1.197 %, respectively.

Heat sources in metallic screens are assumed to be zero due to the bonding design of metallic screens, and therefore this study does not deal with this kind of thermal modeling. Also, consideration of these heat sources would require significant space, which would significantly expand this paper. How to model losses in metallic screens of power cables can be found in [12, 15], or in many other literary sources.

4.4 Checking the Accuracy of a FEM-Based Model

In order to ensure the independence of FEM-based steady-state thermal analyses from the number of nodes or finite elements, that is, from the FE mesh density, the conductor temperatures at the axes of the three phase cables must be tracked. Here, the FE mesh independence tests were performed in accordance with [8, 18]. The FE mesh density was varied from the FE mesh density corresponding to automatic mesh generation to the FE mesh densities corresponding to the first and second mesh refinements. First, the FEM-based model from Figure 2(a) with dimensions of 10 m × 5 m was tested, followed by the one from Figure 2(b) with dimensions of 40 m × 21.5 m. Both models were analyzed for the case of Scenario A. Table 2 outlines the results of FE meshes independence (convergence) tests performed using the FEM-based models from Figures 2(a) and 2(b) for Scenario A.

For the case of the small-size computational domain, the following maximum conductor temperatures were obtained: 92.323 °C – after automatic generation, 92.328 °C – after the first refinement, and 92.328 °C – after the second refinement. The differences between these temperatures were lower than 0.01 °C, but this does not mean that the FEM-based model with dimensions of 10 m × 5 m provided an accurate solution. According to Table 2, this is because the deviation of the maximum conductor temperature from the corresponding continuously permissible temperature T_{cp} is +2.328 °C. Here, it is required that the maximum conductor temperature must be approximately equal to the temperature T_{cp}. In addition, for the large-size computational domain, the following maximum conductor temperatures were calculated: 90 °C – after automatic generation, 90.008 °C – after the first refinement, and 90.009 °C – after the second refinement. In this case, the differences between the maximum conductor temperatures and the corresponding deviation were lower than 0.01 °C. Accordingly, in the case of the large-size computational domain, the variations in the FE mesh density could not affect the conductor temperature and the corresponding ampacity. Therefore, the mesh with the FE density corresponding to the automatic mesh generation provided accurate steady-state temperature distributions.

5 Conclusion

This paper proposed solutions to address some of the gaps in the technical report IEC TR 62095, which refer to single-core power cables with XLPE insulation installed directly in the dried-out soil, in trefoil formation. The key conclusions that emerged from the conducted FEM-based steady-state thermal analyses are the following:

- In relation to an underground cable line installed at a standard depth, the left-hand, bottom and right-hand edges of an appropriate computational domain should be positioned at a distance of 20 m each, which in this particular case resulted in the computational domain having dimensions of 40 m × 21.5 m.
- For an underground cable line installed at a depth

approximately equal to or greater than ten times the outer cable diameter, the ground surface should be modeled with a boundary condition of constant temperature equal to the reference soil temperature, while the left-hand, bottom and right-hand edges of the computational domain should be modeled with an adiabatic boundary condition.

- If the ground surface above an underground cable line is grey, coated or cool, then it can be modeled with an appropriate combination of forced convection and radiation boundary conditions.
- It is important to ensure that longitudinal power losses in conductors, insulation layers and metallic screens of an underground cable line remain unchanged when calculating the corresponding volume powers of heat sources based on the geometric cross-sectional areas of the cable construction elements.
- When verifying the accuracy of any FEM-based steady-state thermal model with underground power cables, the effect of the FE mesh density on the maximum conductor temperature should be analyzed in relation to the corresponding continuously permissible temperature.
- The accuracy of the results obtained using the FEM was successfully verified by the results of calculations based on the relevant IEC standards.
- The FEM-based steady-state thermal models used showed the same level of conservatism as the corresponding IEC 60287-based models and provided the results that are on the side of safety, which obviously cannot affect associated design costs.

Finally, future research will deal with other recommendations from the technical report IEC TR 62095 that require amendment proposals and scientific analysis. Specifically, future research should include the sizing of computational domains, specification of boundary conditions, modeling of heat sources, and verification of the accuracy for the purposes of FEM-based dynamic thermal models of underground power cables in various formations for cyclic and emergency ampacities. In addition to this, some specific examples from practice will be solved analytically and numerically.

Data Availability Statement

Data will be made available on request.

Funding

This work was a part of the research conducted within the projects No. NIO 200132, NIO 200155 and NIO 200148 supported by the Ministry of Education, Science and Technological Development of the Republic of Serbia.

Conflicts of Interest

The authors declare no conflicts of interest.

Ethical Approval and Consent to Participate

Not applicable.

References

[1] *Finite element analysis for cable rating calculations*. (2025, May 26). Online Library for Electrical Power Systems Publications | eCIGRE. Retrieved from https://www.e-cigre.org/publications/detail/963-finite-element-analysis-for-cable-rating-calculations.html#pSummary

[2] *IEC 60287-1-1:2023 cmv*. (n.d.). IEC WebstoreIEC. Retrieved from https://webstore.iec.ch/en/publication/85666

[3] *IEC 60287-2-1:2023 cmv*. (n.d.). IEC WebstoreIEC. Retrieved from https://webstore.iec.ch/en/publication/85669

[4] *IEC 60287-3-1:2017 rlv*. (n.d.). IEC WebstoreIEC. Retrieved from https://webstore.iec.ch/en/publication/60845

[5] *IEC TR 62095:2003*. (n.d.). IEC WebstoreIEC. Retrieved from https://webstore.iec.ch/en/publication/6455

[6] Kim, Y. S., Cong, H. N., Dinh, B. H., & Kim, H. K. (2025). Effect of ambient air and ground temperatures on heat transfer in underground power cable system buried in newly developed cable bedding material. *Geothermics, 125*, 103151. [CrossRef]

[7] Bustamante, S., Mínguez, R., Arroyo, A., Manana, M., Laso, A., Castro, P., & Martinez, R. (2019). Thermal behaviour of medium-voltage underground cables under high-load operating conditions. *Applied Thermal Engineering, 156*, 444–452. [CrossRef]

[8] Klimenta, D., Perović, B., Klimenta, J., Jevtić, M., Milovanović, M., & Krstić, I. (2018). Modelling the thermal effect of solar radiation on the ampacity of a low voltage underground cable. *International Journal of Thermal Sciences, 134*, 507–516. [CrossRef]

[9] Riba, J.-R., & Llauradó, J. (2022). A model to calculate the current–temperature relationship of insulated and jacketed cables. *Materials, 15*(19), 6814. [CrossRef]

[10] Ainhirn, F., Woschitz, R., & Bolzer, A. (2019, June). Extended approach for calculating thermal stress and

ampacity of high voltage cable systems based on experimental data. In *Jicable 2019: 10th International Conference On Insulated Cables*.

[11] Charerndee, K., Chatthaworn, R., Khunkitti, P., Kruesubthaworn, A., Siritaratiwat, A., & Surawanitkun, C. (2020, July). Investment Cost Analysis with Structural Design of Concrete Duct Bank Power Cables. In *IOP Conference Series: Materials Science and Engineering* (Vol. 897, No. 1, p. 012007). IOP Publishing. [CrossRef]

[12] Šućurović, M., Klimenta, D., & Tasić, D. (2024). Correction of the Iec Formula for the Eddy-Current Loss Factor: the Case of Single-Core Cables in Trefoil Formation With Metallic Screens Bonded and Earthed At One End. *Facta Universitatis, Series: Electronics and Energetics*, *37*(2), 391-408. [CrossRef]

[13] Aegerter, D. (2023, June 18–22). Calculation of cable thermal rating using a hybrid method based on IEC 60287 and finite element method. In *Proceedings of the 11th International Conference on Insulated Power Cables (Jicable'23)* (pp. 1–5).

[14] COMSOL. (2012). *COMSOL multiphysics user's guide* (Version 4.3) [Computer software]. COMSOL Inc.

[15] Klimenta, D. O., Perovic, B. D., Jevtic, M. D., Radosavljevic, J. N., & Arsic, N. B. (2014). Thermal FEM-based procedure for design of energy-efficient underground cable lines. *Humanities and Science University Journal Technics*, (10), 162-188.

[16] *IEC 60228:2023 cmv*. (n.d.). IEC WebstoreIEC. Retrieved from https://webstore.iec.ch/en/publication/90329

[17] Heinhold, L. (1991). *Power cables and their application — Part 1* (3rd rev. ed.). Siemens Aktiengesellschaft.

[18] Salata, F., De Lieto Vollaro, A., & De Lieto Vollaro, R. (2015). A model for the evaluation of heat loss from underground cables in non-uniform soil to optimize the system design. *Thermal Science, 19*(2), 461–474. [CrossRef]

Dardan Klimenta was born in Serbia, in 1975. He graduated from the Faculty of Electrical Engineering, University of Priština, in 1998. Also, he received his postgraduate M.Sc. and Ph.D. in 2001 and 2007, respectively, from the Faculty of Electrical Engineering, University of Belgrade. His main research interests include electrical power cable engineering, renewable energy sources, electric power system components, heat transfer, optimization methods, FEM and FEA. Currently, he is a Full Professor with the Faculty of Technical Sciences, University of Priština in Kosovska Mitrovica. (Email: dardan.klimenta@pr.ac.rs)

Marko Šućurović was born in Serbia, in 1988. He received his B.Sc. and M.Sc. in 2011 and 2012, respectively, from the Faculty of Technical Sciences in Čačak, University of Kragujevac. Also, he is a Ph.D. student at the Faculty of Electronic Engineering, University of Niš. His main research interests include electrical power cable engineering, renewable energy sources, electric power system components, heat transfer, FEM and FEA. Currently, he is a Teaching and Research Assistant with the Faculty of Technical Sciences in Čačak, University of Kragujevac. (Email: marko.sucurovic@ftn.kg.ac.rs)

Dragan Tasić was born in Serbia, in 1961. He graduated from the Faculty of Electrical Engineering, University of Belgrade, in 1986. Also, he received his postgraduate M.Sc. in 1991 from the Faculty of Electrical Engineering, University of Belgrade, and Ph.D. in 1997 from Faculty of Electronic Engineering, University of Niš. His main research interests include electrical power cable engineering, renewable energy sources, electric power system modeling and analysis, heat transfer and optimization methods. Currently, he is a Full Professor with the Faculty of Electronic Engineering, University of Niš. (Email: dragan.tasic@elfak.ni.ac.rs)